Cooperative Catalysis

Deutsche Ausgabe: DOI: 10.1002/ange.201810891
Internationale Ausgabe: DOI: 10.1002/anie.201810891

Substrate-Induced Self-Assembly of Cooperative Catalysts

Pablo Solís Muñana[+], Giulio Ragazzon[+], Julien Dupont, Chloe Z.-J. Ren, Leonard J. Prins, and Jack L.-Y. Chen**

Abstract: *Dissipative self-assembly processes in nature rely on chemical fuels that activate proteins for assembly through the formation of a noncovalent complex. The catalytic activity of the assemblies causes fuel degradation, resulting in the formation of an assembly in a high-energy, out-of-equilibrium state. Herein, we apply this concept to a synthetic system and demonstrate that a substrate can induce the formation of vesicular assemblies, which act as cooperative catalysts for cleavage of the same substrate.*

Supramolecular chemistry is transitioning from the study of systems under thermodynamic or kinetic control towards the study of systems that operate out-of-equilibrium.[1,2] These systems require the continuous consumption of energy to keep the functional high-energy state populated.[3,4] Compared to systems at equilibrium, this offers exciting new possibilities for the development of molecular machines, smart materials and complex reaction networks.[3–6] Energy dissipating processes play a key role in living organisms, for example, for controlling the structure and dynamics of the cytoskeleton,[7,8] and have recently also been linked to evolutionary processes.[9] This has sparked strong interest in the design of chemical-fuel driven out-of-equilibrium systems, in particular related to self-assembly.[3,10–12] The majority of reported examples rely on the covalent modification of building blocks, which changes their propensity to form assemblies.[13–24] However, driven self-assembly processes in Nature, that is, fuel-driven processes that lead to a population of a high-energy state,[12] rely exquisitely on the use of noncovalent interactions for building block activation.[7] This provides advantages typically associated with molecular recognition processes, such as high selectivity and fast activation rates. It is exemplified by microtubule formation (Figure 1 a), which initiates with the activation of tubulin dimers for self-assembly upon complexation with guanosine triphosphate (GTP).[8] Critically, tubulin dimers act also as a catalyst for the hydrolysis of GTP to GDP, and importantly, catalysis is significantly accelerated in the assembled

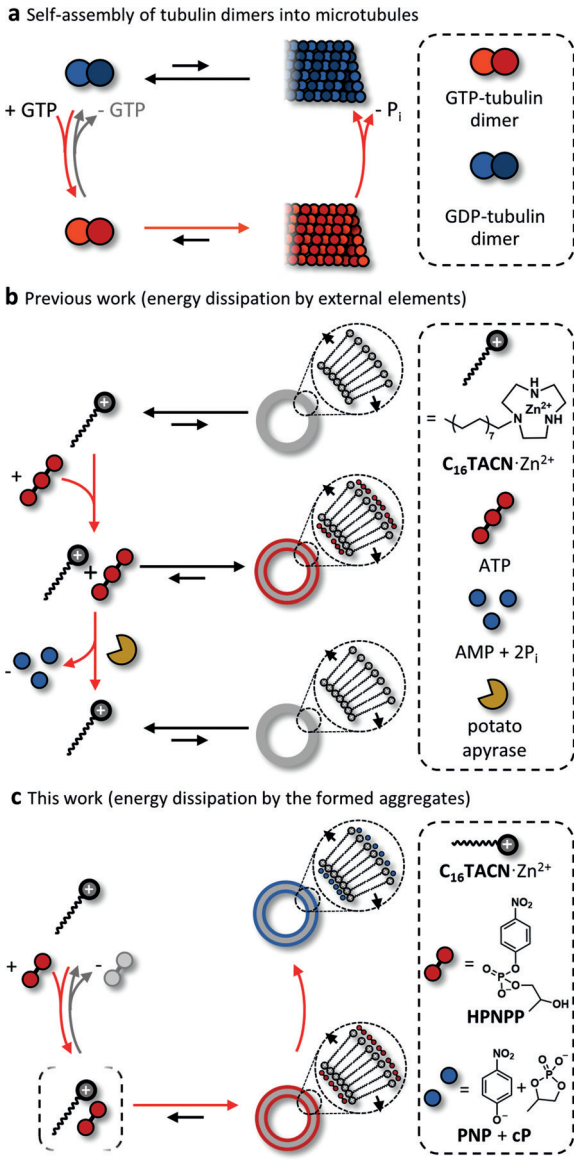

Figure 1. Reaction schemes of non-equilibrium systems; in all figures the red arrows indicate the preferred reaction pathway. a) Reaction scheme for the dissipative formation of microtubules. Guanosine triphosphate (GTP) activates tubulin towards self-assembly and the enhanced catalytic activity in the assembled states affords a high-energy tubular structure. b) Example of the commonly used strategy for the formation of noncovalent assemblies under dissipative conditions: a high-energy small molecule (here adenosine triphosphate, ATP) templates the assembly of vesicular structures, but is subsequently consumed in an independent process (here as a consequence of the enzymatic hydrolysis of ATP by potato apyrase) reverting the system to its initial state. c) Reaction scheme investigated in the present work: hydroxypropyl *p*-nitrophenyl phosphate (**HPNPP**) templates the formation of assemblies that act as cooperative catalysts for its transphosphorylation.

[*] P. Solís Muñana,[+] J. Dupont, C. Z.-J. Ren, Dr. J. L.-Y. Chen
School of Sciences, Auckland University of Technology
Private Bag 92006, Auckland 1142 (New Zealand)
E-mail: jack.chen@aut.ac.nz
Dr. G. Ragazzon,[+] Prof. L. J. Prins
Department of Chemical Sciences, University of Padova
Via Marzolo 1, 35131 Padova (Italy)
E-mail: leonard.prins@unipd.it
[+] These authors contributed equally to this work.
Supporting information and the ORCID identification number(s) for the author(s) of this article can be found under https://doi.org/10.1002/anie.201810891.

state.[25,26] This leads to formation of a GDP-rich high-energy structure which collapses when the stabilizing caps are lost.[27]

Synthetic chemical-fuel driven self-assembly processes have been reported that also rely on noncovalent interactions between the building blocks and a chemical fuel.[28–38] However, while most cases allude to similarities with microtubule formation or related biological dissipative processes, it turns out that in all the cases reported so far, a fundamentally different mechanism is operative (Figure 1b).[28–38] Contrary to what happens in Nature, energy dissipation, intended as the release of energy stored in the chemical fuel, is not catalysed by the building blocks, but rather by external elements such as an enzyme. This difference is of crucial importance, as to chemically drive an assembly process away from equilibrium using a chemical fuel, two fundamental prerequisites are that (1) the fuel-to-waste conversion is catalysed by the building blocks and that (2) fuel conversion is more efficient in the assembled state. These insights have emerged from a recent theoretical analysis of chemical-fuel driven self-assembly processes.[12]

Numerous research groups are currently pursuing synthetic dissipative self-assembly processes that mimic by design the mechanism of microtubules.[16,21,23,30,33] The system that comes closest to meeting the above-cited criteria is reported by Otto et al. whom described the substrate-induced structural reconfiguration of a dynamic covalent library in favour of the library component best adapted to catalyse the conversion of the substrate.[15] Herein we show, to the best of our knowledge, the first example of substrate-induced templation of a noncovalent assembly, which simultaneously acts as a catalyst for its cleavage by exhibiting cooperativity. This represents the first steps in the operating scheme of the driven self-assembly of microtubules (Figure 1c).

We recently demonstrated that the assembly behaviour of amphiphiles can be regulated by the addition of small oligoanions.[30,31] Amphiphilic **C_{16}TACN**·Zn^{2+} (Figure 1b), containing Zn^{2+}-complexed 1,4,7-triazacyclononane (TACN) head groups were observed to form stabilised vesicular assemblies in the presence of ATP. These studies relied on the ability of charged counterions to effectively stabilize the assembly of surfactants containing charged head groups.[39–41] Such counterions have been shown to significantly decrease the critical assembly concentration (cac) of amphiphiles in

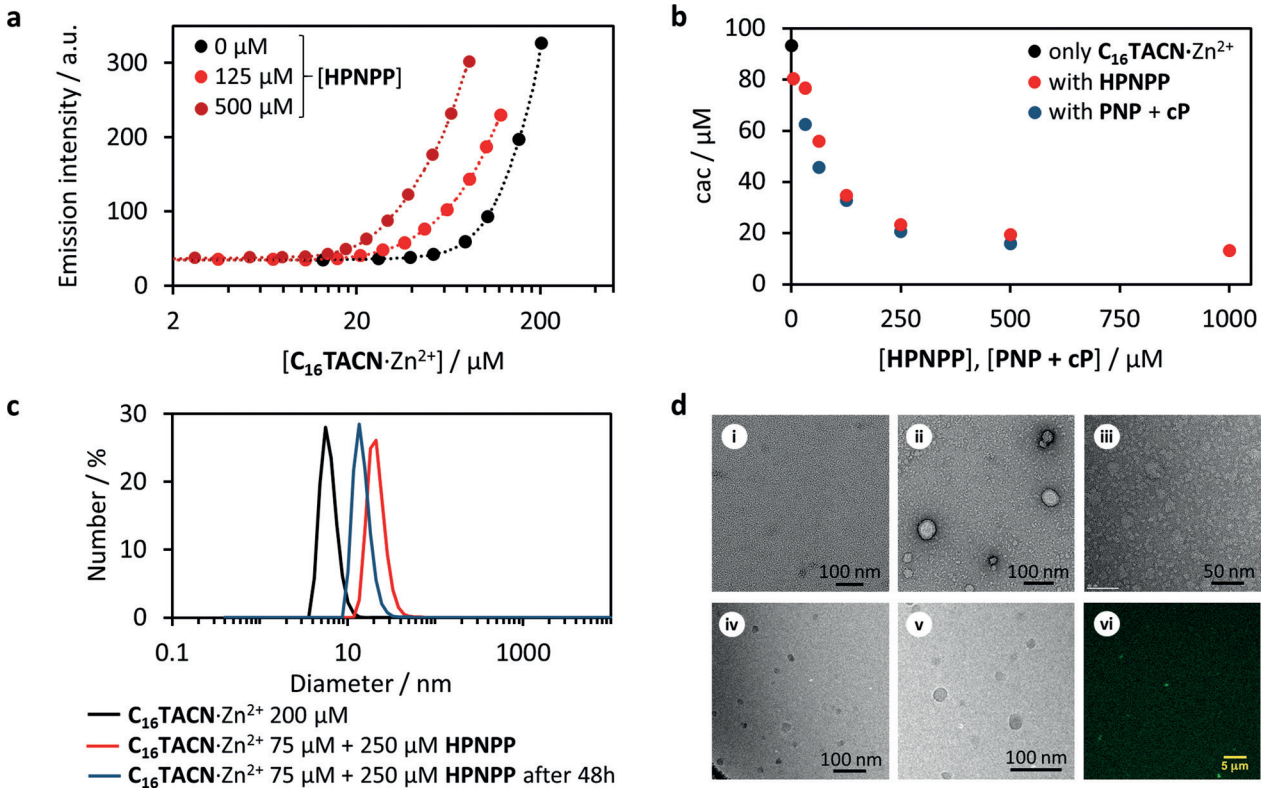

Figure 2. HPNPP templating ability. a) Selected emission intensity profiles for Nile red (5 μM, λ_{ex} = 570 nm, λ_{em} = 643 nm) at increasing **C_{16}TACN**·Zn^{2+} concentrations, in the absence (black dots) and in the presence of **HPNPP** (125 μM, light red dots and 500 μM, dark red dots); the dotted lines serve as guide for the eye; b) Critical assembly concentration of **C_{16}TACN**·Zn^{2+} measured in the presence of different concentrations of **HPNPP** or waste products (**PNP** + **cP**) with Nile red as a fluorescent probe. c) Hydrodynamic diameter of assemblies measured with dynamic light scattering (DLS) in the absence of **HPNPP** (black line) and in the presence of **HPNPP** (red line) and in the presence of waste (**PNP** + **cP**). d) Representative transmission electron microscopy (TEM) images of (i) [**C_{16}TACN**·Zn^{2+}] = 50 μM in the absence of substrate **HPNPP**; (ii) vesicles obtained with [**C_{16}TACN**·Zn^{2+}] = 50 μM in the presence of **HPNPP** (250 μM) and (iii) structures formed with [**C_{16}TACN**·Zn^{2+}] = 50 μM in the presence of waste; (iv) and (v) show representative cryoTEM images with [**C_{16}TACN**·Zn^{2+}] = 50 μM and [**HPNPP**] = 250 μM; (vi) shows a representative image of vesicles with confocal microscopy for samples prepared with [**C_{16}TACN**·Zn^{2+}] = 75 μM, [**HPNPP**] 250 μM and [coumarin 153] = 1 μM. All experiments were performed in aqueous buffer solution (HEPES, 10 mM, pH 7.0) at 25 °C and standard TEM images were stained with 1% uranyl acetate solution.

solution.[30,31,39] Importantly, the TACN·Zn^{2+} moiety featured in the above studies has also been utilised as catalysts for the cleavage of phosphodiester bonds.[42–44] This transphosphorylation reaction is known to require at least two metal ions acting cooperatively to achieve productive levels of activity. Manea et al. demonstrated that the complexation of Zn^{2+} by TACN units immobilised on the surface of gold nanoparticles allows cooperativity to occur between proximal catalytic moieties, leading to remarkable efficiencies in the cleavage of phosphate esters.[42] These nanoparticles covered with an organic monolayer of TACN·Zn^{2+} groups have been termed "nanozymes", as they possess many key features of natural enzymes, including Michaelis–Menten kinetics and cooperativity.[42,45] Our goal was to investigate whether these two effects—templation and catalysis—could be combined in a single system in which the phosphodiester substrate would induce assembly of TACN·Zn^{2+}-containing amphiphiles, and in this way, also generate the catalyst for its destruction (Figure 1c). The model substrate typically used in the study of RNA phosphodiester hydrolysis is 2-hydroxypropyl *p*-nitrophenyl phosphate (**HPNPP**).[42,43] **HPNPP** is negatively charged and contains a phosphate group which we have shown previously to exhibit high affinities for the TACN·Zn^{2+} moiety.[46] We thus had reason to believe that **HPNPP** would be able to act as an efficient counterion and to have a significant effect on the assembly behaviour of **C_{16}TACN**·Zn^{2+}. The cac of **C_{16}TACN**·Zn^{2+} in the absence of substrate was first measured by titrating increasing amounts of the surfactant to an aqueous solution buffered at pH 7.0 containing the fluorescent apolar probe Nile red (5 μM, λ_{ex} = 570 nm, λ_{em} = 643 nm). This probe is solubilised by the apolar compartment of the assemblies, leading to an increase in fluorescence intensity after the cac has been reached (Figure 2a). The cac was determined to be approximately 93 μM under these conditions, which is in close agreement with previous studies.[30] The cac was next determined in the presence of different concentrations of **HPNPP** substrate. Figure 2b shows the significant decrease in the cac of **C_{16}TACN**·Zn^{2+} with increasing concentrations of **HPNPP**. The initial drop in cac is steep, with substrate binding shifting the cac down to 34 μM in the presence of 125 μM of **HPNPP**. Further increases in the concentration of **HPNPP** resulted in additional decreases in the cac, eventually levelling off at around 13 μM in the presence of 1 mM of **HPNPP**. The decrease in cac demonstrates that the presence of **HPNPP** increases the thermodynamic stability of the formed assemblies. The induced formation of assemblies below the native cac was further supported by dynamic light scattering (DLS) experiments, in which assemblies of 24 ± 15 nm were detected (Figure 2c). Objects of comparable size were also observed by (cryo) transmission electron microscopy (TEM/cryoTEM) and scanning laser confocal microscopy images (Figure 2d), supporting the fact that **HPNPP** promotes the formation of vesicular assemblies.

Satisfied that the substrate was effective in promoting assembly, we proceeded to examine the ability of the formed assemblies to promote catalysis. Using **HPNPP** as the substrate, the transphosphorylation reaction results in the formation of a cyclic phosphate (**cP**) and the release of *p*-nitrophenolate (**PNP**), which allows the reaction rate to be conveniently measured spectrophotometrically. Figure 3b shows a plot of the initial rates of reaction with varying concentrations of **C_{16}TACN**·Zn^{2+} in the presence of **HPNPP** (62 μM) in aqueous buffer ([HEPES] = 10 mM, pH 7). At low concentrations of **C_{16}TACN**·Zn^{2+} (0–50 μM), very low reaction rates are observed. At a concentration of around 50 μM,

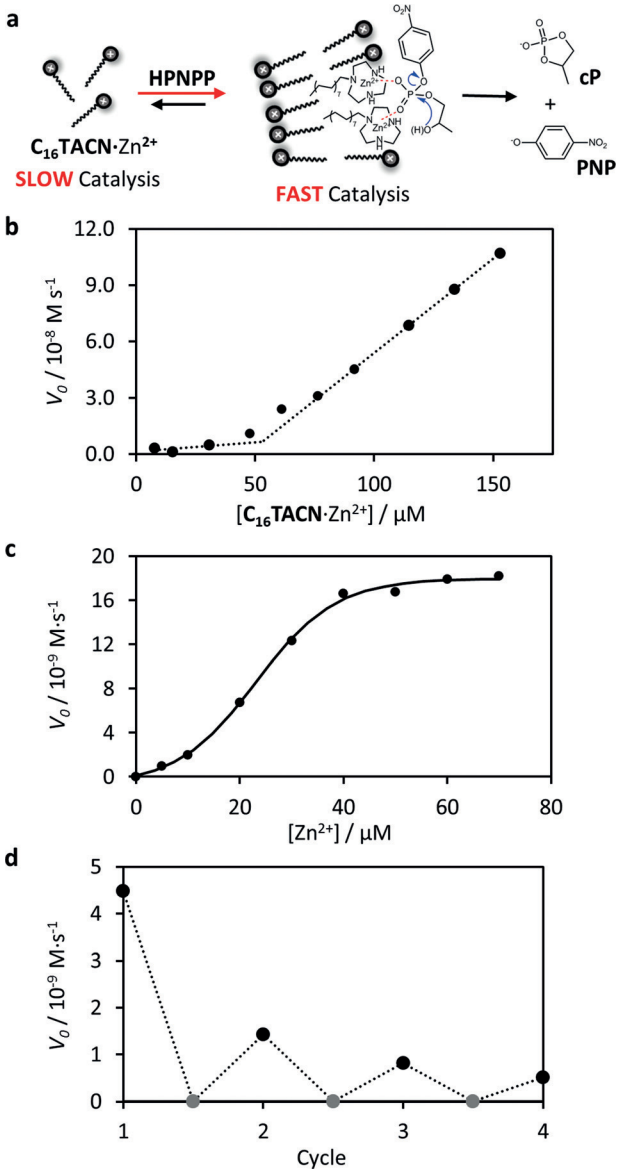

Figure 3. a) Cooperative catalysis induced by neighbouring **TACN**·Zn^{2+} complexes upon assembly. b) Initial speed of **HPNPP** hydrolysis at increasing **C_{16}TACN**·Zn^{2+} concentrations ([**HPNPP**] = 62 μM), the dotted lines are the linear fit to the first three and last three data points. c) Initial speed of **HPNPP** hydrolysis at a fixed concentration of **C_{16}TACN** and varying Zn^{2+} concentrations ([HEPES buffer] = 5 mM, [**C_{16}TACN**] = 50 μM, [**HPNPP**] = 500 μM, 40 °C); the solid line represents the sigmoidal fit of the experimental data. d) Initial rates of **HPNPP** hydrolysis after successive additions of **HPNPP** (125 μM each addition) in the presence [HEPES buffer] = 5 mM and [**C_{16}TACN**·Zn^{2+}] = 50 μM at 40 °C. Black data points represent the rate directly after each addition, Grey data points represent the rate after 48 hours just before addition of the new batch of fuel.

however, the measured initial rates started to increase significantly, with the reaction rate being directly proportional to the surfactant concentration. Several important conclusions can be drawn from this experiment. The observation that the change of slope is observed at a concentration (54 μM), which closely matches the cac under these conditions (≈55 μM, see SI, section 4b), indicates that assembly formation facilitates catalysis. In addition, comparison of the slopes below and above the cac shows that the assemblies have a significantly higher activity compared to the monomeric surfactant. The significant rate enhancement upon assembly-formation is confirmed by additional studies that are described below. Independent evidence for catalysis was obtained from ^{31}P-NMR spectroscopy. A fixed amount of **C_{16}TACN**·Zn^{2+} (75 μM) was added to a constant concentration of **HPNPP** (1.0 mM) and changes in the ^{31}P NMR spectra were monitored as a function of time (see SI, section 4c). The intensity of the signal due to **HPNPP** (−5.69 ppm) decreases, while a new signal at 17.14 ppm originating from the cyclic phosphate waste product appears.

The observed rate acceleration upon assembly strongly suggests that a cooperative mechanism is operative (Figure 3a), similar to that observed previously in catalytic nanoparticles containing the same TACN·Zn^{2+} complex. Strong support that this is indeed the case came from a study in which the transphosphorylation activity of the assemblies was measured in the presence of varying concentrations of Zn^{2+} ions (Figure 3c). Experiments were performed at 50 μM of surfactant and 500 μM of **HPNPP**, at conditions where the system is in the assembled state both in the presence and absence of Zn^{2+} ions (see SI, section 4d). The sigmoidal curve observed for the initial rate as a function of Zn^{2+} concentration is characteristic of cooperative catalysis by metal centres.[42,43] At low concentrations of Zn^{2+} metal ions (up to around 30 mol% saturation of the head groups) low reaction rates are observed, because of the low number of catalytic pockets formed by neighbouring Zn^{2+} complexes. At higher Zn^{2+}-loadings, the amount of catalytic pockets rapidly increases and, consequently, the rate increases significantly until a maximum is reached when the system is fully saturated with Zn^{2+} ions.

The observation of cooperative catalysis by **C_{16}TACN**·Zn^{2+} assemblies was not an obvious result. Indeed, it had been previously reported that an analogous surfactant with a shorter chain showed very low catalytic activity for the same reaction, which was attributed to the highly dynamic nature of the assemblies.[42] To investigate this aspect in more detail, we decided to prepare and study a series of surfactant molecules with hydrophobic chains of varying lengths, from ethyl (**C_2TACN**) through to stearyl (**C_{18}TACN**) as the kinetic stability of surfactant-based assemblies is known to increase with the lengthening of the alkyl chain.[47,48] Figure 4a shows the transphosphorylation activity at different concentrations of surfactants and equimolar Zn^{2+} in a buffered solution containing excess **HPNPP** (500 μM). Analysis of the data shows, as expected, a general increase in reaction rate with increasing concentrations of C_nTACN·Zn^{2+}. However, differences in reactivity of multiple orders of magnitude are observed between catalysts with hydrophobic chains of different lengths measured at the same head group concentration. For example, the rate of reaction with **C_{18}TACN**·Zn^{2+} is roughly double the rate of reaction with **C_{16}TACN**·Zn^{2+} at 100 μM, which is over a magnitude higher than that of **C_{14}TACN**·Zn^{2+} (note the logarithmic scale on both axes). At the same concentration, the activities of **C_{12}TACN**·Zn^{2+} or **C_2TACN**·Zn^{2+} were negligible. Importantly, comparison of the onset of catalytic activity with the cac value (42 μM) of **C_{14}TACN**·Zn^{2+} in the presence of 500 μM **HPNPP** confirms that assembly is a prerequisite for observing catalysis (see SI, section 4e for details). Indeed, the poor catalytic activity of **C_{12}TACN**·Zn^{2+} and **C_2TACN**·Zn^{2+} is in agreement with the fact that these surfactants do not assemble at the concentration regime studied.

Interestingly, one might expect the reaction rates to be in a similar range for the different catalysts once the cac is reached, as above these concentrations similar assemblies are expected to be formed. Yet, the observed large difference between for example **C_{14}TACN**·Zn^{2+} and **C_{18}TACN**·Zn^{2+} indicates clearly that this is not the case. To gain further insight into this difference, the catalytic activity of **C_{18}TACN**·Zn^{2+} and **C_{16}TACN**·Zn^{2+} was measured at varying concentrations of **HPNPP** (Figure 4b). Fitting of the satu-

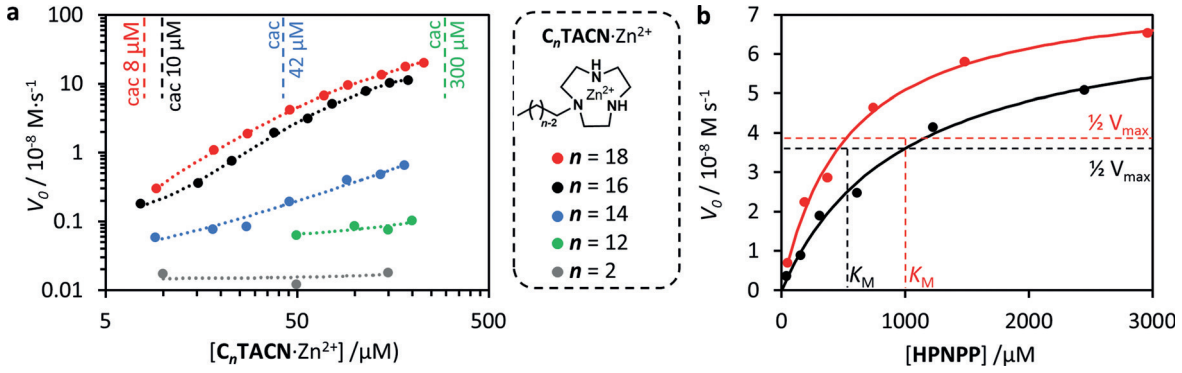

Figure 4. Effect of chain length on catalytic activity. a) Initial speed of **HPNPP** hydrolysis at increasing **C_nTACN**·Zn^{2+} concentration (n = 2 to 18, see legend, [**HPNPP**] = 500 μM, [HEPES buffer] = 5 mM), the dotted lines serve as a guide for the eye. b) Initial speed of **HPNPP** hydrolysis at increasing **HPNPP** concentration, and fixed **C_nTACN**·Zn^{2+} concentration ([**C_nTACN**·Zn^{2+}] = 50 μM, [HEPES buffer] = 50 mM), the solid line are the data fit according to a Michaelis–Menten mechanism. Experiments were performed in aqueous buffer at pH 7, at 40°C.

ration profiles to the Michaelis–Menten equation yielded similar V_{max} values for $\mathbf{C_{18}TACN}{\cdot}Zn^{2+}$ ($7.8 \pm 0.3 \times 10^{-8}$ mol s^{-1}) and $\mathbf{C_{16}TACN}{\cdot}Zn^{2+}$ ($7.2 \pm 0.6 \times 10^{-8}$ mol s^{-1}), but a significantly lower K_M value for $\mathbf{C_{18}TACN}{\cdot}Zn^{2+}$ (0.53 ± 0.06 mM) compared to $\mathbf{C_{16}TACN}{\cdot}Zn^{2+}$ (1.0 ± 0.1 mM). The nearly identical V_{max} values indicate that no intrinsic difference exists between the catalytic pockets in the formed assemblies, whereas the different K_M values indicate that the difference originates from the binding interaction between the surfactants and **HPNPP**. It is important to emphasize that, in contrast to a regular covalent catalyst such as an enzyme or nanozyme, in this system the substrate also affects the amount of catalyst present by acting on the equilibrium between monomeric and assembled states. The observation that the cac values in the presence of the same amount of **HPNPP** are inversely correlated to the hydrophobicity of the surfactant, implies that a higher amount of catalyst is present at the same concentration of **HPNPP**. This explains the higher observed rate at lower substrate concentrations and, consequently, the difference in apparent K_M. Taken together, the three-order of magnitude increase in activity upon self-assembly (comparing $\mathbf{C_{18}TACN}{\cdot}Zn^{2+}$ and $\mathbf{C_2TACN}{\cdot}Zn^{2+}$) suggests that the enhanced activity with increasing the chain length could arise from the thermodynamic interplay between the surfactant and the substrate.

The fate of the self-assembled structures following **HPNPP** hydrolysis was investigated by observing samples after 48 h, when nearly all of the **HPNPP** had been converted to **cP** and **PNP**. Data from both DLS and TEM experiments revealed the presence of assemblies that were smaller in size than in the presence of **HPNPP** (see Figure 2c, 2d(iii)). The observation that the waste products of **HPNPP** cleavage are able to stabilise the formation of assemblies was supported by measuring the cac of the system in the presence of **cP** and **PNP** (see Figure 2b). These experiments suggest that **cP** and **PNP** have similar affinity for the assemblies as the substrate **HPNPP**. Regrettably, it implies that in the current system we are not able to observe the spontaneous dissociation of assembled structures after fuel consumption. Yet, this state is still a responsive one as shown by refuelling experiments in which successive batches of chemical fuel are added at 48 h intervals (Figure 3d). The catalytic activity can be reactivated, but with successively lower rates due to the build-up of waste products which compete with the **HPNPP** substrate for binding to the surface of the assembled structures. This shows that binding is reversible and that the catalyst does not become irreversibly inhibited by the accumulated waste.

This study highlights the importance of cooperative catalysis for the design of energy driven processes. We have demonstrated the substrate-induced self-assembly of a supramolecular cooperative catalyst, a common mechanism of action in natural systems, that has so far not been exploited in synthetic systems.[7,12] In analogy with microtubule formation, the substrate promotes the formation of a noncovalent assembly and activates a cooperative catalytic pathway leading to its degradation. Cooperativity is connected to the assembled state and is able to induce rate accelerations of multiple orders of magnitude. The cooperative catalytic mechanism demonstrated is of utmost importance for the development of dissipative self-assembling systems as it provides a tool to install kinetic asymmetry in energy consumption pathways.[12] It paves the way for the preparation of high-energy assemblies through energy-dissipating processes and eliminates the necessity for external elements to dissipate energy. It is important to note that the substrate-induced self-assembly of cooperative catalysts is also exploited in natural systems for regulatory purposes, including the activation of protease caspase-1[49] and of the main protease of SARS coronavirus,[50] which points to a common underlying mechanism widely exploited by nature. Current efforts are aimed at developing alternative substrates with substantially higher affinity for the catalyst compared to the waste products which would cause spontaneous disassembly after fuel-to-waste conversion.

Acknowledgements

Financial support from a Catalyst: Seeding Grant (CSG-AUT1701) from the Royal Society of New Zealand and New Zealand's Ministry of Business, Innovation and Employment and the European Research Council (ERC StG 239898) is acknowledged. We thank Dr Adrian Turner for assistance with TEM imaging, Dr Ilaria Fortunati for the confocal microscopy images, and Sushmitha Chandrabhas for carrying out preliminary experiments.

Conflict of interest

The authors declare no conflict of interest.

Keywords: amphiphiles · biomimetic catalysis · cooperative catalysis · dissipative self-assembly · systems chemistry

How to cite: *Angew. Chem. Int. Ed.* **2018**, *57*, 16469–16474
Angew. Chem. **2018**, *130*, 16707–16712

[1] B. A. Grzybowski, W. T. S. Huck, *Nat. Nanotechnol.* **2016**, *11*, 585–592.
[2] E. Mattia, S. Otto, *Nat. Nanotechnol.* **2015**, *10*, 111–119.
[3] S. A. P. van Rossum, M. Tena-Solsona, J. H. van Esch, R. Eelkema, J. Boekhoven, *Chem. Soc. Rev.* **2017**, *46*, 5519–5535.
[4] G. Ashkenasy, T. M. Hermans, S. Otto, A. F. Taylor, *Chem. Soc. Rev.* **2017**, *46*, 2543–2554.
[5] S. Kassem, T. van Leeuwen, A. S. Lubbe, M. R. Wilson, B. L. Feringa, D. A. Leigh, *Chem. Soc. Rev.* **2017**, *46*, 2592–2621.
[6] R. Merindol, A. Walther, *Chem. Soc. Rev.* **2017**, *46*, 5588–5619.
[7] B. Alberts, A. Johnson, J. Lewis, M. Raff, K. Roberts, P. Walter, *Molecular Biology of the Cell*, *4th ed.*, Garland, New York, **2002**.
[8] H. Hess, J. L. Ross, *Chem. Soc. Rev.* **2017**, *46*, 5570–5587.
[9] J. L. England, *Nat. Nanotechnol.* **2015**, *10*, 919–923.
[10] F. Della Sala, S. Neri, S. Maiti, J. L.-Y. Chen, L. J. Prins, *Curr. Opin. Biotechnol.* **2017**, *46*, 27–33.
[11] S. De, R. Klajn, *Adv. Mater.* **2018**, *30*, 1706750.
[12] G. Ragazzon, L. J. Prins, *Nat. Nanotechnol.* **2018**, *13*, 882–889.
[13] J. Boekhoven, A. Brizard, K. Kowlgi, G. Koper, R. Eelkema, J. van Esch, *Angew. Chem. Int. Ed.* **2010**, *49*, 4825–4828; *Angew. Chem.* **2010**, *122*, 4935–4938.

[14] A. K. Dambenieks, P. H. Q. Vu, T. M. Fyles, *Chem. Sci.* **2014**, *5*, 3396 – 3403.
[15] H. Fanlo-Virgós, A. R. Alba, S. Hamieh, M. Colomb-Delsuc, S. Otto, *Angew. Chem. Int. Ed.* **2014**, *53*, 11346 – 11350; *Angew. Chem.* **2014**, *126*, 11528 – 11532.
[16] J. Boekhoven, W. Hendriksen, G. Koper, R. Eelkema, J. van Esch, *Science* **2015**, *349*, 1075 – 1079.
[17] M. Tena-Solsona, B. Rieß, R. Grötsch, F. Löhrer, C. Wanzke, B. Käsdorf, A. Bausch, P. Mueller-Buschbaum, O. Lieleg, J. Boekhoven, *Nat. Commun.* **2017**, *8*, 15895.
[18] L. S. Kariyawasam, C. S. Hartley, *J. Am. Chem. Soc.* **2017**, *139*, 11949 – 11955.
[19] M. Sawczyk, R. Klajn, *J. Am. Chem. Soc.* **2017**, *139*, 17973 – 17978.
[20] A. Sorrenti, J. Leira-Iglesias, A. Sato, T. M. Hermans, *Nat. Commun.* **2017**, *8*, 15899.
[21] B. G. P. van Ravensteijn, W. E. Hendriksen, R. Eelkema, J. H. van Esch, W. K. Kegel, *J. Am. Chem. Soc.* **2017**, *139*, 9763 – 9766.
[22] H. Che, S. Cao, J. C. M. van Hest, *J. Am. Chem. Soc.* **2018**, *140*, 5356 – 5359.
[23] I. Colomer, S. M. Morrow, S. P. Fletcher, *Nat. Commun.* **2018**, *9*, 2239.
[24] M. Tena-Solsona, C. Wanzke, B. Riess, A. R. Bausch, J. Boekhoven, *Nat. Commun.* **2018**, *9*, 2044.
[25] T. David-Pfeuty, H. P. Erickson, D. Pantaloni, *Proc. Natl. Acad. Sci. USA* **1977**, *74*, 5372 – 5376.
[26] M. Caplow, J. Shanks, *J. Biol. Chem.* **1990**, *265*, 8935 – 8941.
[27] H. Bowne-Anderson, M. Zanic, M. Kauer, J. Howard, *Bioessays* **2013**, *35*, 452 – 461.
[28] C. Pezzato, L. J. Prins, *Nat. Commun.* **2015**, *6*, 7790.
[29] C. S. Wood, C. Browne, D. M. Wood, J. R. Nitschke, *ACS Cent. Sci.* **2015**, *1*, 504 – 509.
[30] S. Maiti, I. Fortunati, C. Ferrante, P. Scrimin, L. J. Prins, *Nat. Chem.* **2016**, *8*, 725 – 731.
[31] J. L. Y. Chen, S. Maiti, I. Fortunati, C. Ferrante, L. J. Prins, *Chem. Eur. J.* **2017**, *23*, 11549 – 11559.
[32] F. della Sala, S. Maiti, A. Bonanni, P. Scrimin, L. J. Prins, *Angew. Chem. Int. Ed.* **2018**, *57*, 1611 – 1615; *Angew. Chem.* **2018**, *130*, 1627 – 1631.
[33] S. Dhiman, A. Jain, S. J. George, *Angew. Chem. Int. Ed.* **2017**, *56*, 1329 – 1333; *Angew. Chem.* **2017**, *129*, 1349 – 1353.
[34] S. Dhiman, A. Jain, M. Kumar, S. J. George, *J. Am. Chem. Soc.* **2017**, *139*, 16568 – 16575.
[35] X. Hao, W. Sang, J. Hu, Q. Yan, *ACS Macro Lett.* **2017**, *6*, 1151 – 1155.
[36] A. Mishra, D. B. Korlepara, M. Kumar, A. Jain, N. Jonnalagadda, K. K. Bejagam, S. Balasubramanian, S. J. George, *Nat. Commun.* **2018**, *9*, 1295.
[37] G. Wang, J. Sun, L. An, S. Liu, *Biomacromolecules* **2018**, *9*, 2542 – 2548.
[38] E. Del Grosso, A. Amodio, G. Ragazzon, L. J. Prins, F. Ricci, *Angew. Chem. Int. Ed.* **2018**, *57*, 10489 – 10493; *Angew. Chem.* **2018**, *130*, 10649 – 10653.
[39] R. Sasaki, S. Murata, *Langmuir* **2008**, *24*, 2387 – 2394.
[40] Z. Köstereli, K. Severin, *Chem. Commun.* **2012**, *48*, 5841 – 5843.
[41] G. C. Li, S. Y. Zhang, N. J. Wu, Y. Y. Cheng, J. S. You, *Adv. Funct. Mater.* **2014**, *24*, 6204 – 6209.
[42] F. Manea, F. B. Houillon, L. Pasquato, P. Scrimin, *Angew. Chem. Int. Ed.* **2004**, *43*, 6165 – 6169; *Angew. Chem.* **2004**, *116*, 6291 – 6295.
[43] G. Zaupa, C. Mora, R. Bonomi, L. J. Prins, P. Scrimin, *Chem. Eur. J.* **2011**, *17*, 4879 – 4889.
[44] B. Gruber, E. Kataev, J. Aschenbrenner, S. Stadlbauer, B. König, *J. Am. Chem. Soc.* **2011**, *133*, 20704 – 20707.
[45] H. Wei, E. Wang, *Chem. Soc. Rev.* **2013**, *42*, 6060 – 6093.
[46] C. Pezzato, P. Scrimin, L. J. Prins, *Angew. Chem. Int. Ed.* **2014**, *53*, 2104 – 2109; *Angew. Chem.* **2014**, *126*, 2136 – 2141.
[47] H. Hoffmann, *Ber. Bunsen-Ges.* **1978**, *82*, 988 – 1001.
[48] R. Zana in *Encyclopedia of Surface and Colloid Science*, *2nd ed.*, *Vol. 5* (Ed.: A. T. Hubbard), Taylor & Francis, New York, **2002**.
[49] D. Datta, C. L. McClendon, M. P. Jacobson, J. A. Wells, *J. Biol. Chem.* **2013**, *288*, 9971 – 9981.
[50] S. Cheng, G. Chang, C. Chou, *Biophys. J.* **2010**, *98*, 1327 – 1336.

Manuscript received: September 21, 2018
Accepted manuscript online: October 10, 2018
Version of record online: November 15, 2018

